Landscape Ecol
DOI 10.1007/s10980-015-0219-z

RESEARCH ARTICLE

Linking metrics of landscape pattern to hydrological process in a lotic wetland

Jing Yuan · Matthew J. Cohen · David A. Kaplan · Subodh Acharya · Laurel G. Larsen · Martha K. Nungesser

Received: 17 July 2014 / Accepted: 18 May 2015

Abstract
Context Strong reciprocal interactions exist between landscape patterns and ecological processes. In wetlands, hydrology is the dominant abiotic driver of ecological processes and both controls, and is controlled, by vegetation presence and patterning. We focus on binary patterning in the Everglades ridge-slough landscape, where longitudinally connected flow, principally in sloughs, is integral to landscape function. Patterning controls discharge competence in this low-gradient peatland, with important feedbacks on hydroperiod and thus peat accretion and patch transitions.
Objectives To quantitatively predict pattern effects on hydrologic connectivity and thus hydroperiod.
Methods We evaluated three pattern metrics that vary in their hydrologic specificity. (1) Landscape discharge competence considers elongation and patch-type density that capture geostatistical landscape features. (2) Directional connectivity index (DCI) extracts both flow path and direction based on graph theory. (3) Least flow cost (LFC) is based on a global spatial distance algorithm strongly analogous to landscape water routing, where ridges have higher flow cost than sloughs because of their elevation and vegetation structure. Metrics were evaluated in comparison to hydroperiod estimated using a numerically intensive hydrologic model for synthetic landscapes. Fitted relationships between metrics and hydroperiod for synthetic landscapes were extrapolated to contemporary and historical maps to explore hydroperiod trends in space and time.
Results Both LFC and DCI were excellent predictors of hydroperiod and useful for diagnosing how the modern landscape has reorganized in response to modified hydrology.
Conclusions Metric simplicity and performance indicates potential to provide hydrologically explicit, computationally simple, and spatially independent predictions of landscape hydrology, and thus effectively measure of restoration performance.

J. Yuan (✉)
School of Natural Resources and Environment, University of Florida, 327 Newins-Zeigler Hall, PO Box 110410, Gainesville, FL 32611, USA
e-mail: yj@ufl.edu

M. J. Cohen · S. Acharya
School of Forest Resources and Conservation, University of Florida, 328 Newins-Ziegler Hall, PO Box 110410, Gainesville, FL 32611-0410, USA

D. A. Kaplan
Department of Environmental Engineering Sciences, University of Florida, 6 Phelps Lab, PO Box 116350, Gainesville, FL 32611, USA

L. G. Larsen
Department of Geography, University of California, 507 McCone Hall, Berkeley, CA 94720-4740, USA

M. K. Nungesser
Everglades Systems Assessment Section, South Florida Water Management District, 3301 Gun Club Rd., West Palm Beach, FL 33406, USA

Published online: 29 May 2015

Keywords Spatial metrics · Connectivity · Hydrology · Hydroperiod · Ridge and slough · Wetland · Everglades

Introduction

A fundamental tenet of landscape ecology is that spatial patterns and ecological processes and functions are coupled (Turner et al. 2001; Wu and Hobbs 2002). Hydrology is among the primary drivers of ecological processes in wetlands (Bullock and Acreman 1999; D'Odorico et al. 2010, 2011), shaping landform, transporting nutrients and other solutes, and controlling temporal and spatial patterns of vegetation composition, productivity, and organic matter accretion. However, hydrology is not simply a boundary condition to which the landscape responds. Vegetation in particular can strongly influence hydrology, creating feedbacks (via flow occlusion, evaporative gradients, changes in bed friction, changes in water storage) that can, in turn, shape the structure and function of the landscape (Rietkerk and Van de Koppel 2008).In many patterned wetlands, where vegetation self-organizes into geometrically structured mosaics of patches [e.g., boreal (Eppinga et al. 2008) and subtropical (Larsen et al. 2007; Watts et al. 2010) peatlands], these feedbacks between vegetation and hydrology are of paramount importance for understanding pattern genesis and maintenance (Eppinga et al. 2009; Cohen et al. 2011), and thus also for landscape management and restoration (Suding et al. 2004).

One important challenge in assessing impacts to wetland landscapes (e.g., in response to hydrologic modification and/or restoration activities) is to explicitly account for the strong reciprocal relationships between vegetation and hydrology in measures of landscape pattern. While there are myriad metrics and spatial indices for assessing landscape pattern (e.g., based on patch composition and configuration or on interpolation of continuous variables (Gustafson 1998; McGarigal et al. 2002), the sensitivity and specificity of these metrics to the links between vegetation pattern and hydrologic function, particularly in lotic wetlands, remains unexplored. As such, they are likely unable to successfully enumerate underlying ecological processes in these systems (Turner 1989).

This limitation of existing pattern metrics is apparent in the ridge and slough landscape mosaic in the Everglades (Florida, USA), where a century of hydrologic intervention (flow modification through drainage, compartmentalization, and impoundment) has substantially degraded landscape pattern (SCT 2003). The striking pattern present in the historical landscape and in remnant blocks of the contemporary system consists of elongated sawgrass (*Cladium jamaicense*) patches (ridges) occupying elevations currently 20–30 cm higher (Watts et al. 2010; McVoy et al. 2011; Aich et al. 2013) than the mosaic of interconnected deeper-water sloughs containing a variety of submerged (e.g., *Utricularia* spp., *Myriphylum spicatum*), floating leaved (e.g., *Nymphaea odorata*) and emergent vegetation (e.g., *Panicum hemitomon, Eleocharis elongata*). While both patch types are markedly elongated in the direction of historical water flow, it is the deeper water sloughs which stay almost continuously inundated, and which convey most (ca. 86 %) of the water through the landscape (Harvey et al. 2009). Multiple proposed mechanisms for creation and maintenance of the ridge-slough landscape generate anisotropic directional patterning (Ross et al. 2006; Larsen et al. 2007; Larsen and Harvey 2010; Cheng et al. 2011; Cohen et al. 2011; Heffernan et al. 2013). Until recently (Larsen et al. 2012), however, none of the landscape pattern metrics used to assess spatial and temporal variation in landscape condition explicitly accounted for longitudinal hydrologic connectivity. Specifically, the explicit link between pattern and hydrology shown in Kaplan et al. (2012) is not clearly enumerated by any existing metrics despite the obvious relevance of that link, and despite important progress towards measuring landscape condition using a small number of simple spatial or statistical metrics (Wu et al. 2006; Watts et al. 2010; Nungesser 2011).

Given the foundational role that hydrology plays in the proposed landscape genesis and maintenance mechanisms, and the enormous hydrologic changes that have occurred in the system over the last 100 years, development of metrics that directly link landscape pattern and hydrologic function are clearly needed. A central objective, therefore, is to identify metrics that capture, to varying degrees, the essential features of flow through the landscape, and compare them. To that end, we selected three wholly different approaches to evaluating flow connectivity. The first

focuses on actual water flows, as enumerated by algorithms that assess resistance to flow or flow cost (Eastman 1990), creating a metric we call the least flow cost (LFC). In this approach, each pixel through which water moves has an associated flow cost, with ridges presenting higher flow costs than sloughs due to higher vegetation density and shallower water depths. A least cost algorithm (Eastman 1989) identifies flow paths that minimize the cumulative costs of movement through a landscape, and, in aggregate, provide a metric of hydrologic connectivity that can account for both direct connectivity through low flow-cost patches but that also include shorter flow paths through high flow-cost patches.

The second uses a promising approach proposed by Larsen et al. (2012) called the directional connectivity index (DCI) which enumerates landscape connectivity based on graph-theory. It measures the strength and directionality of connections between nodes (i.e., vegetation patches). It appears to be diagnostic of degrading ecosystem pattern (Larsen et al. 2012), and is more sensitive to changing conditions in the ridge-slough mosaic than the suite of existing landscape pattern indices. While DCI explicitly considers longitudinal connectivity, the link to hydrologic conveyance has yet to be tested.

Finally we developed a new metric derived from work by Kaplan et al. (2012) who used series of synthetic landscapes with varying patch anisotropy to simulate landscape hydrologic behavior using a 2-D hydrodynamic model (SWIFT2D; Schaffranek 2004). The effect of patch anisotropy on hydroperiod, the dominant variable governing vegetation and peat accretion dynamics in this system (Kaplan et al. 2012), was ecologically significant (e.g., average hydroperiod was ca. 40 days shorter in anisotropic landscapes relative to isotropic landscapes, a four-fold increase in the number of dry days per year). While that work demonstrated the link between pattern and hydrologic function, it also implied that landscape hydrology can be discerned from information about ridge density and patch anisotropy, which together govern landscape discharge competence (LDC), the ability of a landscape to convey water, or the specific discharge (m^3/s per unit width), at a given water stage (Kaplan et al. 2012). As such, we a priori define landscape discharge competence as the ratio of anisotropy (e) to ridge density (%R). Given the reliance to date on patch length-to-width ratios as diagnostic metrics of landscape pattern condition (Nungesser 2011), validating the hydrologic specificity of simple statistical measure like LDC is essential.

The goal of this work was to evaluate these candidate spatial pattern metrics (DCI, LDC and LFC) for their ability to predict the hydrological regime based only on landscape pattern, and thereby explore their specificity for detecting changes in the ecological feedbacks that link pattern and function. The metrics vary in their flowpath specificity, with DCI offering the most explicit test of longitudinal slough connectivity (i.e., the 'microstate' of the landscape pattern), LFC providing an intermediate level of flowpath specificity, and LDC providing information on domain-scale properties (i.e., the 'macrostate' of the landscape pattern). After testing the effectiveness of the three metrics for predicting landscape hydroperiod (Fig. 1; white arrows denoting this first step), we applied them to explore the spatial variation in hydrologic connectivity in the highly altered contemporary landscape, and, using existing landscape maps dating back to 1941 (Nungesser 2011), changes that have occurred in response to over 100 years of hydrologic modification (McVoy et al. 2011) (Fig. 1; dark arrows denoting this second step).

Methods

Study site

Our study site is the Everglades in south Florida, including Water Conservation Areas (WCA) 1, 2 and 3, as well as Shark River Slough in northeastern Everglades National Park (ENP) (Fig. 2). While this entire portion of the Everglades was historically free flowing, it is now a heavily managed system bounded by canals and levees that have significantly altered hydrology, which has in turn led to widespread changes in landscape patterning and vegetation structure. The central part of WCA3 is generally considered the best conserved ridge-slough landscape (SCT 2003; Nungesser 2011), and is referred to hereafter as the reference site. To the north and south of this reference landscape, east–west highways (I-75 to the north, Tamiami Trail to the south), have altered water flow. Locally drier conditions in WCA3-North (upstream of I-75) have favored growth of woody vegetation (principally Carolina willow, *Salix caroliniana*) and the loss of slough habitats due to emergent vegetation

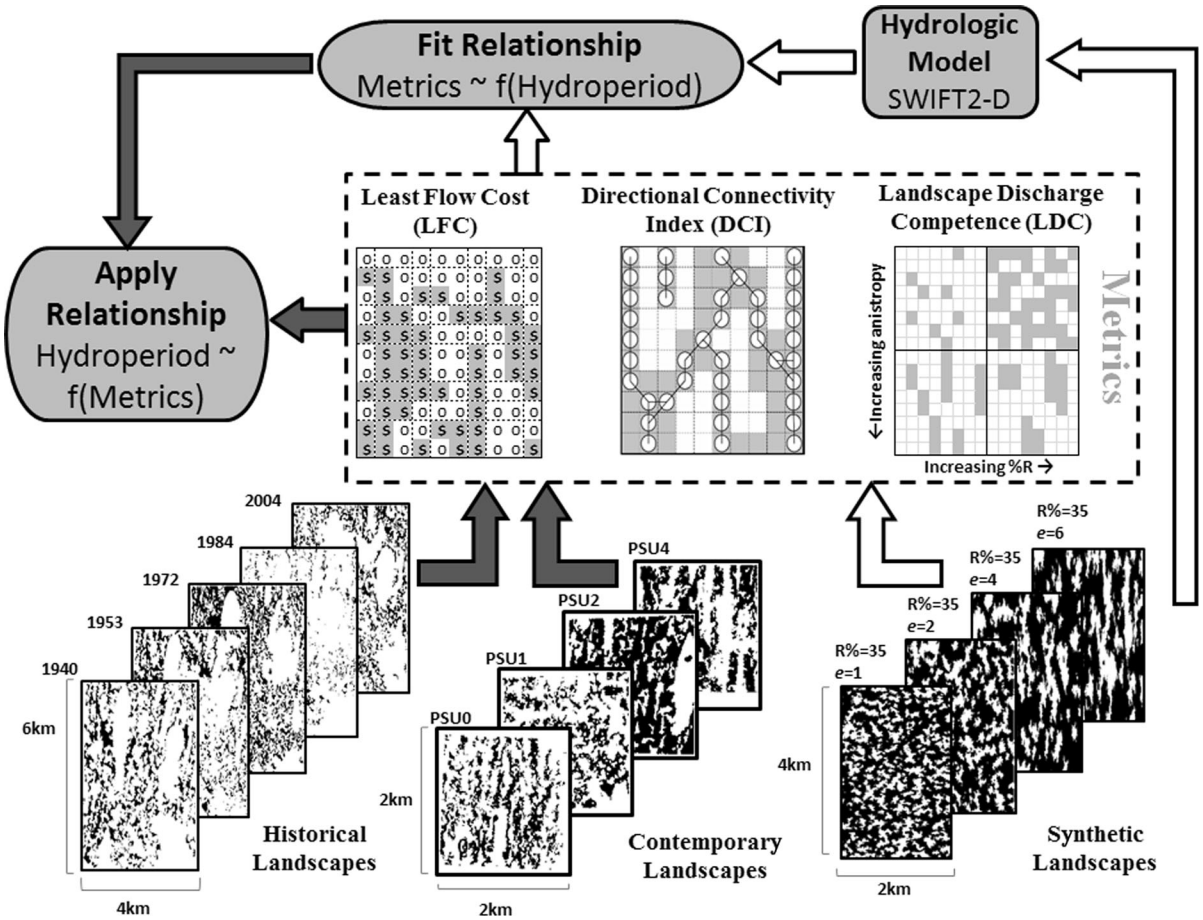

Fig. 1 Schematic of data sources and processes. The three pattern metrics (*dashed box* at *center*) for detecting hydrologic connectivity were directional connectivity index (DCI), landscape discharge competence (LDC), and least flow cost (LFC). The relationship between pattern metrics and hydroperiod (*white arrows*) estimated using a hydrodynamic model (SWIFT2-D) were obtained for synthetic landscapes that varied in ridge density (%R) and anisotropy (e). Based on these fitted relationships, hydroperiod was predicted for free-flowing conditions from contemporary and historical landscapes (*dark arrows*)

encroachment. This process of slough-filling in response to shortened hydroperiod is nearly complete in the northern parts of WCA3A and WCA3B, and is advanced in Everglades National Park (Sklar and van der Valk 2002; Willard et al. 2006). Elsewhere, flow obstruction by Tamiami Trail has impounded water locally upstream (i.e., in southern WCA3), leading to fragmentation and loss of ridges. Large canals (e.g., Miami Canal) route water rapidly from north to south, altering the timing, volume and direction of flows through the ridge-slough mosaic. Elsewhere (e.g., WCA1 and 2), changes in water sources (rainfall vs. canals) and chronic phosphorous (P) enrichment have altered historical biogeochemistry and led to large areas of cattail (*Typha domingensis*) invasions (Reddy et al. 1995; Rutchey and Vilchek 1999; Hagerthey et al. 2008). These changes in natural water delivery (quality and quantity) have a strong effect on vegetation community and structure and thus on pattern. The density of ridges and sloughs, the shapes of individual ridge patches, and the orientation of the patches, which historically was parallel to the flow, have been altered by changing hydrology (Nungesser 2011).

Pattern metrics

To quantify these landscape pattern changes and link them to hydrologic modification, both for understanding ecosystem degradation and also to assess restoration performance, we tested three hydrologically

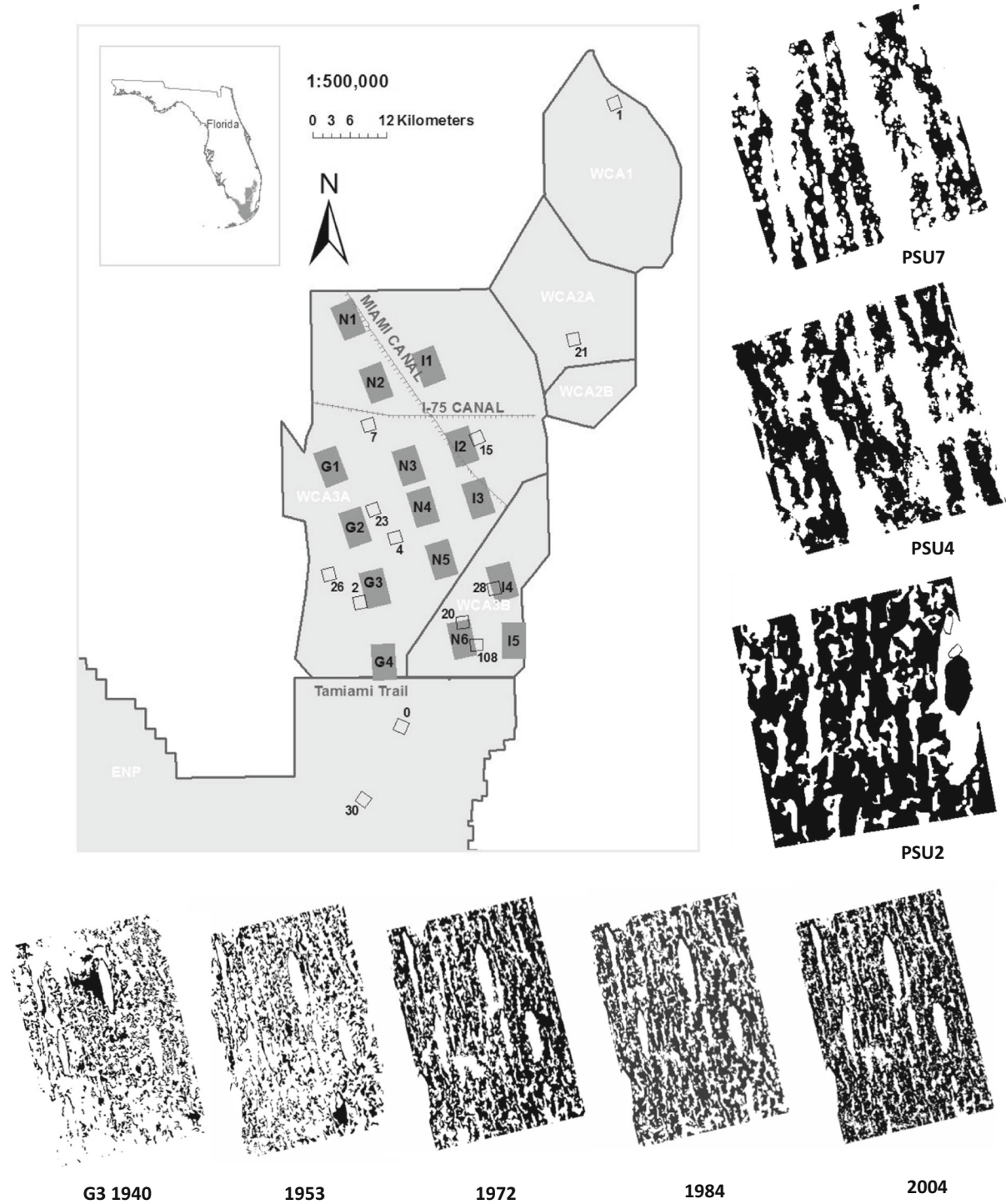

Fig. 2 Research areas and sampling location. Historical vegetation blocks (*dark gray squares* with *G*, *N*, and *I* labels) are 4 × 6 km. The *bottom row* of the image shows temporal changes in vegetation patterning in block G3. Contemporary vegetation blocks (*square outlines*) are 2 × 2 km. The *vertical panel* shows the spatial changes in vegetation pattern along a hydrological gradient, from dry (PSU7) to conserved (PSU 4) to inundated (PSU2). The scales of the depicted contemporary and historical vegetation maps are different in order to show the details of patterning

explicit pattern metrics (Fig. 1; dashed box). We focus specifically on hydroperiod, defined as the portion of a year during which the ridges (high ground) are inundated. A hydroperiod of 1 denotes continuous inundation, while a value of 0.5 denotes ca. 183 days of inundation per year. The broad hydroperiod expectations for ridges (HP $\sim$ 0.85–0.92) and sloughs (HP $\sim$ 0.97–1.0) are derived from hydrologic conditions where the ridge-slough pattern is best conserved (Givnish et al. 2008, Kaplan et al. 2012). We note that there is strong evidence of an optimal hydroperiod for ridges and sloughs in the Everglades, above and below which there is evidence of ecological degradation (Watts et al. 2010).

Least flow cost (LFC)

Passage of any moving agent (water, organisms) through landscapes is subject to friction that controls both the rate and route of movement. A raster based cost-distance procedure (e.g., in Idrisi; Clark Labs, Worcester, MA) produces a continuous surface of cumulative costs with distance from a source location. The cumulative cost is the product of Euclidean distance from a source location and a unit cost per pixel (i.e., friction). For this study, the source is the most upstream row of the domain, and the cumulative costs are assessed based on a raster map of the ridge-slough mosaic with different friction coefficients ascribed to each patch type (ridges > sloughs).

Starting from the top of each domain (i.e., a source row), the cost-push algorithm (Eastman 1989) seeks the lowest cost path through the landscape, with movement in any of 8 directions from a given cell (unit distances in the cardinal directions, and 1.41 units distance in diagonal directions). For each pixel, the resulting value is the cumulative least cost flow-path. We evaluated overall travel costs by averaging values from pixels in the last row, and define the least flow cost (LFC) metric as the ratio of the mean cumulative travel cost to these cells relative to the minimum possible cost (defined by the domain length):

$$\mathrm{LFC} = \frac{1}{m} \cdot \frac{1}{n} \cdot \sum_{1}^{n} C. \quad (1)$$

where m is the domain length (i.e., numbers of rows), n is the number of cells in the bottom row of the domain, and C is the cumulative least flow cost to deliver flow to each of cell at the bottom of the domain, equal to the sum of the flow friction parameter in all cells traversed during passage through the domain. We compared this formulation of LFC (i.e., $\mathrm{LFC_{all}}$) with the flow-cost obtained in the last row for slough pixels only ($\mathrm{LFC_{slough}}$), reasoning that this may better reflect connectivity because most of the flow occurs in sloughs. However, values are effectively identical ($\mathrm{LFC_{all}} = 0.95 \times \mathrm{LFC_{slough}} + 0.06$, $r^2 = 0.99$), suggesting that inferences from LFC are not influenced by this aspect of metric foulation.

In contrast to the pixels selected for LFC estimation, the flow friction parameter appears to be a crucial attribute of this metric. By definition, the friction parameter in sloughs is 1; friction in ridges can be adjusted in accordance with the relative resistance to flow, a parameter roughly analogous to the bed friction (n) in Manning's equation, but with arbitrary units (cost per unit distance) interpreted only in comparison to slough friction. We started with a ridge friction of 5 (i.e., 5 times higher cost than flow in a slough) based on Harvey et al. (2009) who report sloughs route 80-85 % of water through the landscape. However, we investigated ridge friction values ranging from 1.1 to 100, and evaluated concordance between LFC and hydroperiod estimated for the synthetic landscape domains (where hydroperiod is defined as the fraction of time ridges are inundated). Our preliminary analyses showed a sigmoidal relationship between LFC and hydroperiod. For each ridge friction value we obtained the R^2 values as a measure of goodness-of-fit, and selected the final value based on the best fit model (i.e., highest R^2).

Directional connectivity index (DCI)

The directional connectivity index (DCI; Larsen et al. 2012) is a structural connectivity metric that enumerates the linearity of connections in a particular direction (e.g., along a flow path) and has been demonstrated to be closely related to functional connectivity metrics in hydrology. It measures connectivity based on graph theory, wherein "nodes" are defined as all pixels within a skeleton network of a binary image (in which the skeleton represents channel or vegetation patch centers) and "links" denote connections between nodes (Larsen et al. 2012). DCI ranges from 0 (no directional connectivity) to 1 (highly connected and linear in a particular direction),

and can be evaluated using both directed and undirected analyses. With directed analyses, the path connecting any two nodes cannot be routed "upstream" of the starting node, which is appropriate for flow connectivity, and the form we used.

Directional connectivity index (DCI) is defined as:

$$\mathrm{DCI} = \frac{\sum_{i=1}^{v} \sum_{j=r+1}^{R} w_{ij} \frac{dx(j-r)}{d_{ij}}}{\sum_{i=1}^{v} \sum_{j=r+1}^{R} w_{ij}} \quad (2)$$

where i is a node index, j is row index, r is the row containing node i, R is the total number of rows in the direction of interest, v is total number of nodes in the direction of interest, dx is the pixel length, d_{ij} is the shortest path between node i and any node in row j, and w_{ij} is a weighting function that denotes the intended scale of the connectivity assessment (i.e., highly local to increasingly global). Based on Larsen et al. (2012), we adopt a distance-based weight function $w_{ij} = dx(j - r)$, which prioritizes connectivity over the largest scales. We expect that it is the regional-scale interactions between flow and the distribution of resistance elements (i.e., the behavior of flow parcels averaged over many patches) that govern the relationship between connectivity and hydrology, justifying the choice of w_{ij}. As with LFC, we evaluated DCI performance for predicting simulated hydroperiod (see below); preliminary analyses indicated a non-linear association which necessitated comparison of multiple functional forms.

Landscape discharge competence (LDC)

Discharge competence (Kaplan et al. 2012; Heffernan et al. 2013) is the ability of a landscape to convey water, or the specific discharge (m^3/s per unit width) at a given stage. Low discharge competence landscapes require higher water levels to convey the same volume as can be conveyed by landscapes with higher discharge competence. In a patterned wetland, landscape discharge competence (LDC) is dictated by patch density and geometry (Kaplan et al. 2012). A higher density of ridges yields fewer deep and low-friction pathways (sloughs) through the landscape, and reduces discharge competence. Likewise, increasing patch elongation (anisotropy) increases the likelihood of continuous deep, low-friction flowpaths, and thus increases discharge competence. Since discharge competence increases with increased anisotropy of ridge patches and also with decreased ridge density, we define LDC as:

$$LDC = {}^{e}/_{\%R}. \quad (3)$$

where $\%R$ is the density of ridges, and e is the landscape anisotropy (ratio of major to minor semivariogram range). Ridge density was obtained by summing ridge area and dividing by total domain area. Anisotropy was calculated by fitting indicator semivariograms to the binary domains using GSLIB (Deutsch and Journel 1998), and extracting the major and minor ranges. As with the other metrics, we predicted that LDC should be associated with hydroperiod (specifically, that higher LDC results in shorter hydroperiod for a given boundary flow), and evaluated that association using a variety of model functional forms. We note that this particular configuration of two important domain-ale attributes is one among many configurations. This was determined a priori based on findings about the controls on landscape discharge competence on other work (Kaplan et al. 2012; Heffernan et al. 2013), and reflects one plausible description of the 'macrostate' of the system, which stands in contrast to the flowpath specific metrics (DCI and LFC) that assess the 'microstate' of the pattern.

Synthetic, historical and current vegetation maps

We used three sources of landscape vegetation maps (Fig. 1, lower maps). First, to formally explore links between pattern metrics and landscape configuration, we developed a series of synthetic landscapes with varying pattern geometry (maps at right, Fig. 1). Each synthetic domain was 2 × 4 km (elongated in the direction of flow) with two patch types (ridge and slough) differing in elevation by 0.25 m (Watts et al. 2010), and a north–south slope of 3×10^{-5} m/m (Egler 1952). Using sequential indicator simulation in GSLIB (Deutsch and Journel 1998) with a minor range of 100 m (Kaplan et al. 2012), we created 30 replicates at each of seven ridge density levels (%R = 10, 35, 42.5, 50, 57.5, 65 and 90 %) and four anisotropy levels (e = 1, 2, 4 and 6); this resulted in a total of 840 synthetic landscapes. We note that while we imposed simulation constraints on anisotropy, statistical variation unique to each simulation realization leads to actual e values that deviate slightly from the expected

values. All analyses (e.g., computation of LDC) were performed on the actual anisotropy levels (as measured by indicator semi-variograms applied to each synthetic landscape), not the expected level.

Second, to hindcast hydrologic conditions extant in the landscape and examine trajectories of landscape change, we applied the fitted relationships between modeled hydrology (see below) and pattern metrics in these synthetic landscapes to maps derived from imagery between 1940 and the present (maps at left; Fig. 1). Mapping is described in detail in Nungesser (2011); briefly, five aerial images (from 1940, 1953, 1972, 1984 and 2004) were obtained for each of fifteen 4 × 6 km domains spanning a gradient of hydrologic modification. These images were digitized manually into binary vegetation maps. Early maps (1940, 1953 and 1973) were on paper and were scanned to digital files; later maps (1984 and 2004) were digitized from aerial color infrared images. Images from 1984 images had a horizontal resolution of 1.5 m, while 2004 images (Digital Ortho Quarter Quads; DOQQs) had a 1-meter resolution.

Finally, current vegetation maps in eleven 2 × 2 km domains in WCA3 were digitized manually from high-resolution color aerial photographs flown in 2006 and 2009 (maps at center, Fig. 1). For these maps, the minimum mapping unit (MMU) is 400 m^2 (20 × 20 m), with patches classified according to Rutchey et al. (2006). For our analysis, these maps were reclassified into binary classes with all non-slough vegetation coded as ridge. Canals and levees, if present, were cropped to allow pattern analysis.

Since the maps varied in extent and resolution (and thus minimum mapping unit, MMU), we evaluated LFC and LDC performance for different domain sizes and grain sizes; evaluations of scale independence for DCI (Larsen et al. 2012), has previously been performed. Dependency of domain extent was evaluated using vegetation maps that encompass all of Water Conservation Area 3 (WCA3) (Rutchey et al. 2008), derived from hand-digitization of 1:24000 scale color-infrared photographs obtained in 1994 and 1995 into vegetation classes; the minimum mapping unit is one hectare (100 × 100 m). Using a fixed grain size of 10 m, we created a binary (ridge and slough) map and investigated the LFC and LDC metrics in domains of different extent. We started with three 8 × 8 km blocks selected to span the regional gradient in hydrologic condition within WCA3; a drained unit located north of I-75, a flooded unit located north of Tamiami Trail, and a conserved unit located in the center of WCA3. From each block, we randomly selected 20 sub-domains of three sizes (4 × 4, 2 × 2, and 1 × 1 km) for which we calculated the metrics. We compared these results within and across blocks to ensure the metrics consistently captured pattern conditions regardless of domain size. We also evaluated the grain-size dependency of the metrics using maps from three PSUs (2, 4, 7) that span a gradient of condition. These were rasterized at 3, 10, 20, 50 and 100 m pixel resolutions, and the values of LFC and LDC compared between them.

Hydrologic modeling

A spatially explicit numerical model (SWIFT2D; Schaffranek 2004) was used to simulate the hydrologic regime in the synthetic domains following the approach of Kaplan et al. (2012). The model assumes steady flow, a surface water slope that is parallel to the bed slope, a spatially homogenous Manning's roughness coefficient of 0.45, and ridge-slough elevation difference of 25 cm. The model routes water through the domain via fixed-head boundary conditions at the top and bottom of the model domain (no-flow boundary conditions are implemented on the sides of the domain) to develop a stage-discharge relationship (i.e., rating curve) for each synthetic landscape. A reference flow time series was developed in Kaplan et al. (2012) using this approach based on measured stage in a well conserved 2 × 4 km landscape block in the of center WCA3. In this work, the 20-year reference flow time series was used along with domain rating curves to develop a 20-year record of stage in each synthetic domain, which was used to calculate hydroperiod (i.e., percent of time ridges are inundated).

Model fitting

To evaluate their effectiveness for predicting landscape hydroperiod, we regressed each metric against hydroperiod obtained for each of the 840 synthetic landscapes. Several non-linear functions were evaluated including logarithmic, quadratic, cubic, power, and sigmoidal models; we selected the model with the lowest Akaike Information Criterion (AIC) to represent the relationship between landscape metrics and

hydroperiod. AIC measures the relative quality of a statistical model based on the trade-off between the goodness of fit and model complexity (Burnham and Anderson 2002). Using the best fit model and the computed values of the connectivity metrics, we hindcasted hydroperiod for the current and historical landscapes and explored trajectories of landscape changes. The trend of inferred hydroperiod changes from 1940 to 2004 was assessed using linear regression. Because of low samples size for trend detection ($n = 5$ observations in each time series), we adopted a higher significance level ($p \leq 0.1$) when evaluating observed trends. We also applied the metrics to contemporary landscape blocks to evaluate concordance between model predicted hydroperiod and qualitative variation in long term hydrologic changes that have occurred in the landscape.

When evaluating metric performance for estimating hydroperiod, it is important to note that hydroperiods are derived from model simulations not monitored records. More importantly, the metrics predict hydroperiod in a setting without regional hydrologic modification. That is, the hydroperiod predictions are for a free-flowing condition through each landscape block. The presence of levees and canals has radically altered hydrology over large areas, which has led to significant reorganization of vegetation patterning, with areas that have been regionally drained exhibiting loss of sloughs and connectivity, and areas that are impacted by regional impoundment exhibiting fragmentation and reduced area of ridges. However, when those landscapes are evaluated by the metrics, they have properties that would, under free-flowing conditions, yield the opposite hydrology. That is, landscapes where slough area and connectivity have declined would, under free-flowing conditions, have a very long hydroperiod because of poor water routing ability, despite the fact that the regional hydrologic trend that engendered that pattern was too short a hydroperiod. Likewise, landscapes with lower ridge density are that way because of prolonged inundation, but would, under free flowing conditions, have short hydroperiods because the adjusted landscape pattern facilitates flow. This inversion of model predictions vis-à-vis extant hydrologic conditions, with the most well conserved landscapes always intermediate, is extremely important to note when drawing inferences from these metrics.

Results

Effects of anisotropy on hydroperiod

Simulated hydroperiod in the synthetic domains ranged from 0.7 to 1, which means ridges were inundated between 70 and 100 % of the 20 year simulation period. Hydroperiod increased with higher ridge density and decreased with higher anisotropy (Fig. 3). This hydroperiod range aligns with measured values where pattern remains relatively intact (Givnish et al. 2008; Kaplan et al. 2012). Anisotropy effects (i.e., separation between lines in Fig. 3) are highest at intermediate ridge density, suggesting ridge density is the primary control, and anisotropy is a secondary control. Anisotropy and density controls on hydroperiod were previously shown (Kaplan et al. 2012) but only at a ridge density of 50 %.

Friction coefficients for the least flow cost metric and its scale dependency

Based on the best sigmoid model fit (highest R^2) between LFC and hydroperiod for the 840 synthetic domains, the selected flow friction coefficient for ridges was 1.4 (slough friction is defined as 1.0) (Fig. 4). While the model fit is best for surprisingly

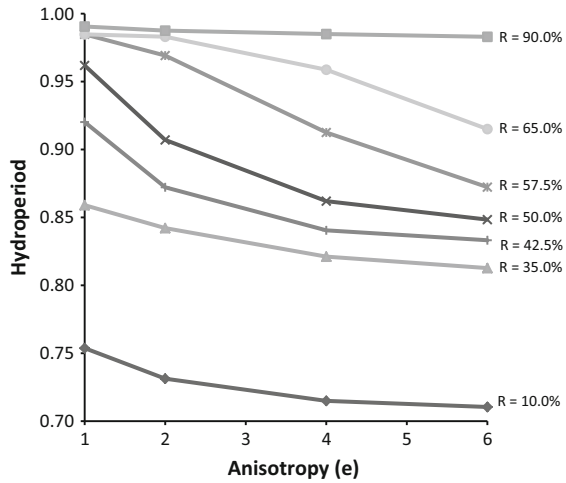

Fig. 3 The effect of ridge density and patch anisotropy on average hydroperiod in synthetic domains. 840 synthetic landscape domains were generated with different patch geometry (seven ridge density levels and four anisotropy levels). Hydroperiod was simulated by the SWIFT2D model, and the average value for each patch geometry is plotted. Hydroperiod increases with ridge density and decreases with anisotropy

small friction values, model performance is roughly equal over a friction parameter range from 1.3 to 5.0.

LDC and LFC were independent of domain extent based on concordance between mean metric values at different extents, and the value obtained from the largest (8 × 8 km) sampling block (Fig. 5). As expected, variance in both LDC and LFC increases with decreasing window size regardless of landscape condition (e.g., drained—Fig. 5a, d, reference—Fig. 5b, e, or impounded—Fig. 5c, f). We note, however, that variation in mean values across window sizes is smaller than variation across domains, suggesting that metrics are robust to differences in domain size between our various map products.

Our evaluation of the grain-size dependence of LDC and LFC (Fig. 5a, b) suggests that values are consistent across pixel sizes up to 20 m, but that anomalies emerge for larger sizes. This principally arises because of the computation of anisotropy (e) which becomes unstable for the largest pixel sizes, where insufficient statistical power arises because lags are constrained by the small domain size (2 × 2 km, yielding a maximum of 20 pixels at 100 m resolution). Judging from the behavior at smaller grain sizes, variation in LDC is acceptable, and LFC is highly predictable (Fig. 6).

Metric performance

The relationship between metrics and simulated hydroperiod in the synthetic domains was strong ($r^2 > 0.6$, $p < 0.0001$) for all three metrics (Fig. 7). LFC was positively associated with hydroperiod and best represented by a sigmoid curve (Fig. 7a, Eq. 4).

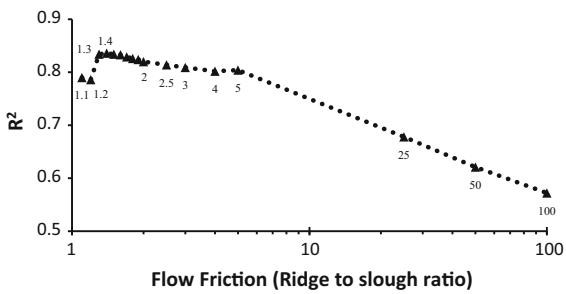

Fig. 4 Model fit (R^2) between the least flow cost (LFC) value and hydroperiod (HP) as a function of the ratio of flow friction coefficients in ridges versus sloughs; an optimal ratio of 1.4 was obtained

DCI was negatively associated with hydroperiod with a cubic model best fit to the observations (Fig. 7b, Eq. 5). LDC was negatively associated with hydroperiod, with the relationship best represented by a power law (Fig. 7c, Eq. 6). However, LFC and DCI outperformed the LDC metric ($R^2 = 0.92$ and 0.88 vs. 0.69, respectively), suggesting that metrics that explicitly account for landscape flowpaths (LFC and DCI) outperform those based on statistical proxies for hydraulic geometry (LDC). We note that the R = 10 % simulations are apparent oers for all metrics. Because ridge densities this low are never found on the contemporary Everglades, we tested the effect of omitting these values from the hydroperiod model fitted. The fit to HP is worse for all models, particularly for the LDC ($r^2 = 0.69$ with the %R = 10 %, $r^2 = 0.52$ without), but the estimated model parameters are identical. As such, we retained the R = 10 % simulations for all three metrics.

$$HP_{LFC} = 1 - \frac{1}{1 + \left(\frac{LFC}{0.96}\right)^{20.1}} \tag{4}$$

$$\begin{aligned} HP_{DCI} &= 0.99 - 0.8 \times DCI \\ &= 1.8 \times DCI^2 - 1.6 \times DCI^3 \end{aligned} \tag{5}$$

$$HP_{LDC} = 0.69 \times LDC^{-0.08} \tag{6}$$

Predictions of contemporary hydrology

Metric predictions of hydroperiod in the contemporary vegetation blocks (labeled triangles in Fig. 7) are sorted in the same way by all three metrics, with three sites (P20, P28, and P108) at the upper end of predicted hydroperiod, two (P2 and P23) at the lower end, and three sites (P0, P4, and P7) consistently in the middle. Note that this sorting is the reverse of observed hydroperiods. As described in the methods, this discrepancy arises because the regression-based prediction of hydroperiod assumes a free flowing system where regional hydrologic changes due to water management infrastructure are absent.

Hindcasting hydroperiod using connectivity metrics

Trends in historical hydroperiod estimates (from Eqs. 4 through 6) were evident in a relatively small number of landscape blocks (12 of 45) (Fig. 8a). The

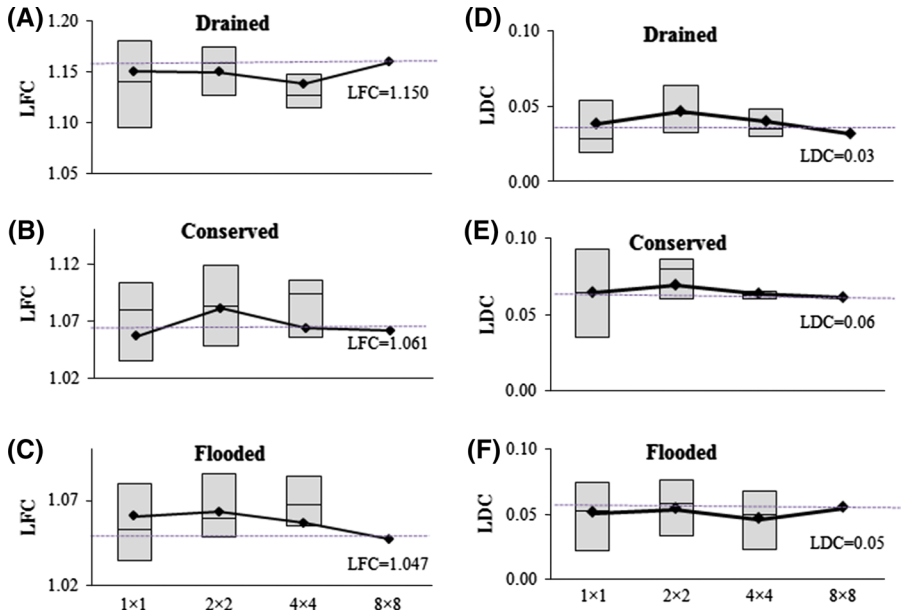

Fig. 5 Metric values for the average least flow cost (LFC) and landscape discharge competence (LDC) depend on the analysis extent. Shown are comparisons of metric values for different analysis extents in drained (*upper*), conserved (*middle*), and flooded (*lower*) sites. As the analysis extent increases, metric variance decreases for both LFC and LDC, but the mean remains stable

low incidence of significant trends is at least partially due to low statistical power, but may also be due to non-monotonic temporal patterns in predicted hydroperiod vary among plots (Fig. 8b). Whereas in some cases there is a clear trend in hydroperiod (e.g., at G3 or N6), in other settings there are substantial changes between years, but no overall trend (e.g., G4 and N4). We note that the decadal hydroperiod change at G3, for example, indicates a progressive decrease, but this site is located in southern WCA3 where regional impoundment (i.e., long hydroperiod) has been persistent. This inversion of actual and estimated hydroperiod, which has been previously mentioned, can be qualitatively corrected by inverting the sign of the change. As such, Fig. 8a depicts the trend of hydroperiod changes as the reverse of slopes from metric regressions (Fig. 7b).

Predictions made by the three metrics are generally well aligned, with many of the same blocks exhibiting significant trends (Fig. 8a), and highly convergent estimates of hydroperiod values and variation (Fig. 8b). LFC and DCI are particularly strongly concordant with the exception of divergence forvplots G1, N4, and I4. At least two metrics support that G3 and N5, for example, have increased hydroperiod (Fig. 8a). Note that decadal-scale trends are not the only changes of interest, or the only ones evident in the half century spanning 1940–2004. In many blocks where long-term hydroperiod trends were not statistically significant from 1940 to 2004, predicted hydroperiod varied dramatically over shorter timescales implying significant plasticity in vegetation patterning. For instance, hydroperiods in G4, N2 and I3 show no significant trend, but do show substantial, but largely incongruent, temporal variability.

Discussion

Comparing metrics of hydrologic connectivity

Evidence of strong links between landscape pattern and hydroperiod (Figs. 3, 7) underscores the importance of metrics that explicitly consider water flow when evaluating landscape changes in response to hydrologic modification. The three metrics selected for analysis (LFC, DCI, and LDC) vary in hydrologic specificity, but all share a core focus on longitudinal flow through complex landscapes. All three metrics are effective at predicting hydroperiod, each

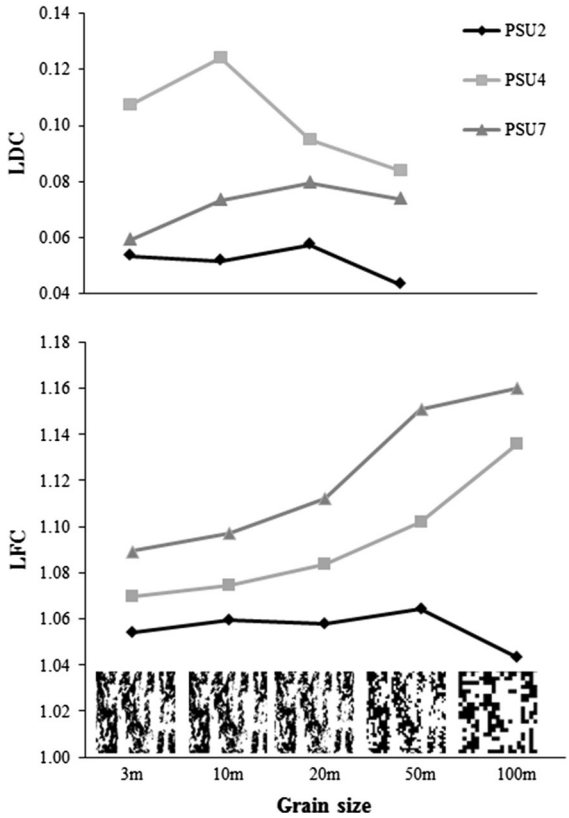

Fig. 6 Metric values for least flow cost (LFC) and landscape discharge competence (LDC) depend on the grain size of the analysis; maps with different pixel sizes (PSU4) are shown below. At pixel sizes 20 m and below, metric values are stable, but large pixel sizes create metric anomalies

explaining over 70 % of variation in hydroperiod across synthetic domains. We note that anisotropy or ridge density, two metrics that have previously been proposed as diagnostic of ridge-slough pattern condition (Wu et al. 2006), and which taken together comprise one of the metrics (LDC) are, on their own, poor predictors of hydroperiod ($r^2 = 0.09$ and 0.4, respectively). Further, other pattern metrics based solely on geometry (e.g., mean ridge width or length, fractal dimension, lacunarity) are also poor predictors of hydroperiod ($r^2 < 0.12$; Yuan 2015), suggesting they fail to capture important features of flow routing in this complex landscapes. While simpler metrics may offer insights on other aspects of landscape function, their utility for diagnosing flow-connectivity is clearly limited compared to the flow-explicit metrics considered here.

While each of the three metrics considered has a strong association with landscape hydroperiod, the direction and functional form of these relationships is not uniform. As expected, higher values of the least flow cost (LFC), which can vary from a minimum of 1 to a maximum defined by the ridge friction coefficient (e.g., 1.4), imply poorer connectivity, and thus longer hydroperiod. What was unexpected was the sigmoidal shape of that relationship, which exhibits a steep increase in hydroperiod as LFC increases even slightly above 1. When LFC reaches 1.1, the turning point indicated by piecewise regression (analysis not shown), hydroperiod approaches 100 % and thus ceases to change; this point occurs in landscapes where the lowest-cost flowpaths contain 25 % ridge pixels. We note that the best-conserved landscape (P4) has an LFC value of 1.07, which predicts ridge hydroperiod of 0.9, strikingly similar to actual hydroperiods in the well-conserved landscape (0.88 over the last 20 years, Kaplan et al. 2012).

Similarly, high DCI values, which range from 0 to 1, and which imply greater regional scale connectivity in the direction of historical flow, correspond with shorter hydroperiods. In contrast, water movement is slowed by high hydraulic resistance and shallow flow in landscapes with low DCI, resulting in hydroperiod near 1. The best-conserved block (P4) has a moderate DCI value (0.334), which predicts a hydroperiod of 0.87, again similar to observed conditions. While overall behavior is reasonable, the hydroperiod versus DCI relationship was nonlinear, with two zones of high sensitivity to DCI change (below 0.2 and above 0.6); at intermediate DCI, hydroperiod is less sensitive to DCI variation. Previous results from ridge-slough landscape simulations suggest that over this range, DCI responds linearly to changes in the number of spanning paths (i.e., connected paths that completely span the model domain), which tend to decrease rapidly with degradation, even as ridge cover remains roughly constant (Larsen et al. 2012). Lack of hydroperiod sensitivity to DCI in this region reflects the fact that hydroperiod responds both to ridge aerial coverage and DCI, and that the relationship between ridge coverage and DCI is nonlinear. Future models may need to account explicitly for the independent effects of ridge coverage and DCI.

Across the real and synthetic landscapes, LDC ranges from 0 to 0.667, but in practice there is no theoretical upper-bound because anisotropy (the nu-

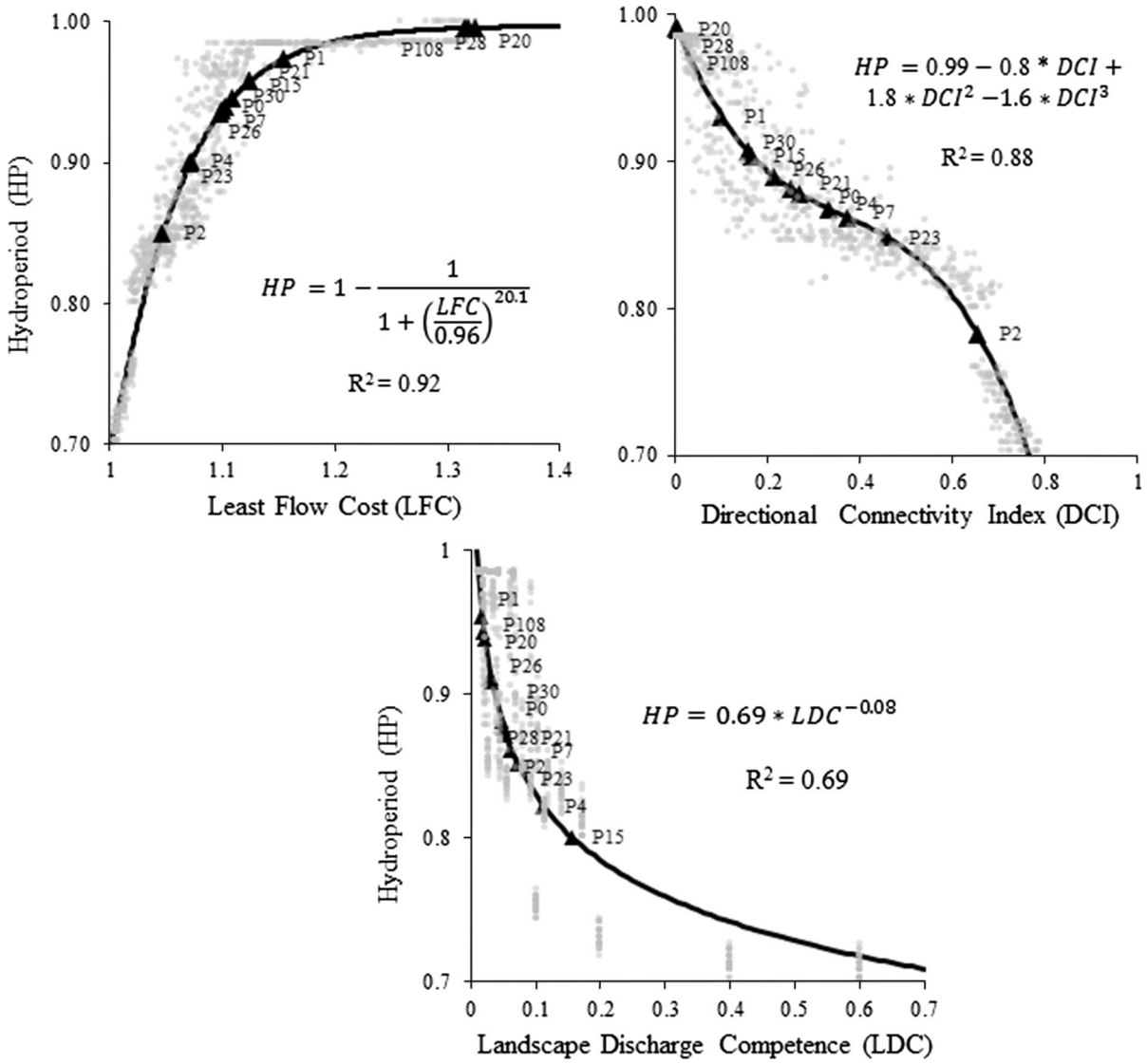

Fig. 7 Regression model fits between landscape metrics and hydroperiod simulated with the SWIFT2D model. *Gray dots* are datasets calculated from 840 synthetic landscapes. *Black lines* are the best fit models. *Black triangle dots* represent the calculated landscape metrics from 11 contemporary vegetation blocks. The hydroperiod for contemporary vegetation blocks is calculated from the best fit regression: **a** sigmoidal, **b** cubic, and **c** power-law

merator) can increase indefinitely and ridge density (the denominator) can approach zero. As expected (Kaplan et al. 2012), increased LDC predicts shortened hydroperiod, and LDC values of 0.11 in the reference landscape correspond to predicted hydroperiod (0.82) similar to observed values. The functional form of hydroperiod versus LDC, like LFC, suggests rapid hydroperiod changes in response to LDC increases when values are low, but convergence on consistent low hydroperiod for LDC > ca. 0.2. This lower hydroperiod bound is controlled by the boundary conditions imposed within the SWIFT2D model, which represents 20 years of observed stage data; while this period included a wide variety of climate conditions, it may not fully represent the long term distribution of hydrologic conditions in the region. Strong non-linearity in the LDC-hydroperiod relationship may have restoration significance, since relatively

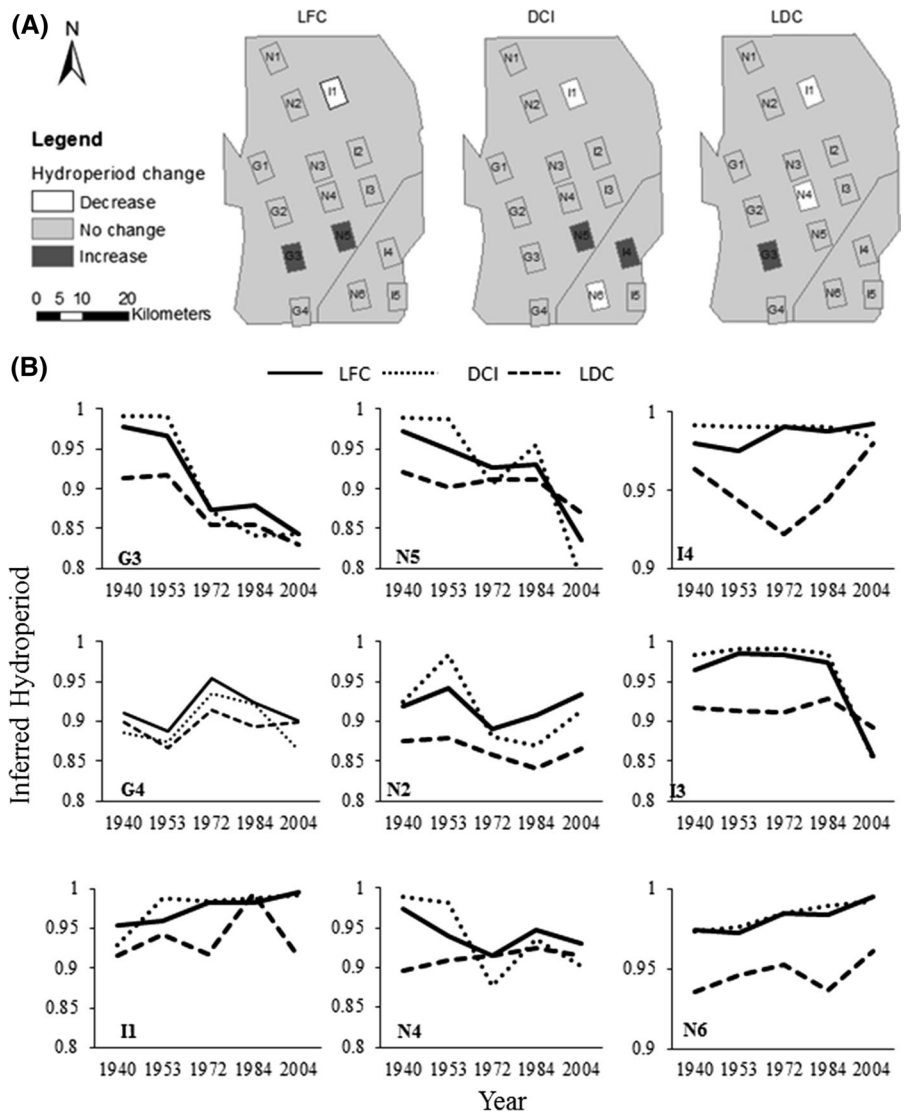

Fig. 8 Hindcast hydroperiods based on regression fits and landscape connectivity metrics computed from historical imagery. *Panel A* shows inferred hydroperiod trends from 1940 to 2004, based on the Mann–Kendall trending test ($p < 0.1$) on predicted eriods. *Dark grey* depicts inferred long-term increases in hydroperiod, whereas white depicts inferred long-term decreases. Places where no significant hydroperiod changes have occurred are shown in the background color. *Panel B* shows the decadal predicted hydroperiod change of selected plots from 1940, 1953, 1972, 1984 and 2004

minor changes in landscape geometry appear to have large impacts on landscape scale hydrologic regime, while smaller changes in hydroperiod occur when the landscape is already substantially modified. Notably, all of the existing landscapes (black triangles in Fig. 6), including those where pattern has markedly changed due to hydrologic modification, exhibit LDC values <0.2 (i.e., where hydroperiod sensitivity to LDC is high).

The construction of the LDC metric (i.e., e: %R) was determined a priori in response to previous work on reciprocal feedbacks between pattern and hydrology (Kaplan et al. 2012; Heffernan et al. 2013). This configuration has certain logical problems, specifically, that the effect of anisotropy (e) is most significant when %R is small. While other configurations of these two domain-scale variables actually provide more successful predictions from a statistical perspective (e.g., a complex 3rd order polynomial used in a model developed in Acharya et al. (in review)), our goal was not to extract a post hoc best fit LDC formulation. Indeed, while we did explore several alternative formulations of LDC (e.g., $e^{R\ \%}$ or e*R %), we found no evidence to supplant the current formulation. Since our goal was centrally to assess the efficacy of a simple 'macro-state' metric

(albeit one informed strongly by theory and simulation modeling), and then contrast this with metrics that explicitly consider flowpaths, or landscape 'microstate', we intentionally avoided more complex empirical functions like those used in Acharya et al. (in review). We also note that some potential artifacts of our a priori LDC formulation are obviated by the absence, in any part of the existing or historic Everglades, of landscapes with ridge densities below 30 %, and further that models relating the existing LDC formulation to HP without the %R = 10 % simulations (i.e., the lowest points in the Fig. 7c) yielded the identical model parameters and slightly weaker fit.

While all three metrics effectively predict variation in hydroperiod, and the best-conserved sites exhibit moderate metric values in all cases, LFC and DCI ($r^2 = 0.92$ and 0.88, respectively) have a stronger relationship than LDC ($r^2 = 0.69$) (Fig. 7). This is partially due to more parameters in the LFC and DCI models (both have 4 while the LDC model only has 2), but in each case we selected the model with the lowest AIC. Another explanation may be the hydrologic specificity of LFC and DCI vis-à-vis LDC. Both of the former metrics explicitly capture flowpaths of hydrologic connectivity, while LDC provides only a statistical proxy for connectivity (Kaplan et al. 2012) that considers the fundamental controls (patch density and geometry) but cannot account for impedance along actual flow paths. This distinction is also manifest in hindcast hydroperiod predictions for historical landscapes, where DCI and LFC make very similar predictions about hydroperiod that often diverge from LDC predictions (Fig. 8).

While it is unlikely that performance differences between LFC and DCI are functionally significant, one reason LFC may slightly outperform DCI may again be related to explicit consideration of resistances along flowpaths. DCI is the mean of the shortest distance between nodes within a specific habitat type; as such, it measures connectedness of continuous flow paths, and not necessarily flow along complex flowpaths that may include other habitat types. In contrast, LFC measures the "quality" of a given flow path by considering aggregate friction, even if the flowpath includes both habitat types. Despite this difference, the success of both DCI and LFC suggest that specifying flow paths is critical for capturing underlying hydrologic process. As such, we conclude these connectivity metrics better reflect the linkage of process and pattern and thus realize the primary objective of pattern metrics (Kupfer 2012).

Feedbacks between vegetation pattern and landscape hydrology

Although landscape pattern metrics have been widely used in conservation planning, the strength of links between pattern metrics and underlying ecological processes have long been challenged (O'Neill et al. 1999; Opdam et al. 2001; Turner et al. 2001; Corry and Nassauer 2005). Where they have been evaluated, landscape metrics developed based on explicit mechanistic considerations capture emergent landscape process better than generic pattern metrics. For example, research on a leakiness index (LI, or directional leakiness index, DLI) that measures how landscapes retain resources outperformed conventional patchiness metrics for diagnosing ecosystem integrity (Tongway and Ludwig 1997; Ludwig et al. 2002). Although DLI is constructed based on simple patch geometry and distance, it predicts landscape function because it considers how spatial configuration of vegetation cover and terrain affect soil loss (Ludwig et al. 2006), rather than more generic features of landscape configuration.

While exogenous changes in hydrology lead to well documented changes ridge slough landscape pattern, the arrangement of patches also exerts a reciprocal effect on hydrology; in short, pattern geometry can alter hydrologic behavior, even where the boundary condition flows are the same (Kaplan et al. 2012). This implies a feedback between pattern and hydrology that may have important implications for the genesis of contemporary pattern geometry. Exploration of this feedback and its impact on the self-organization of the pattern has been the subject of models that explore sediment redistribution in Everglades (Lago et al. 2010; Larsen and Harvey 2010), and has recently been extended to a more explicit consideration of pattern geometry effects on hydroperiod (Acharya et al. in review), with results that suggest that simple rules arising from this coupling of pattern and hydrology can plausibly reproduce the geostatistical patterns of the extant landscape. Our work here strongly supports the reciprocal links between pattern and hydroperiod, and suggests that as the landscape self-organizes in

response to hydrologic drivers, these pattern metrics provide a useful means to assess trajectories.

All three metrics make predictions about pattern effects on hydroperiod in a free-flowing Everglades. That is, landscapes with predicted long hydroperiods have vegetation patterns that inhibit flow, specifically areas where ridge density has increased and/or continuous flowpaths have been removed by changes in patch geometry. These kinds of self-organized changes in patterning are predicted to occur in the actual landscape in response to conditions of prolonged drying (i.e., short hydroperiod). This underscores the two-way nature of the hydrology-vegetation relationship, wherein the landscape pattern self-organizes in response to hydrology, which in turn affects that hydrology. This inversion in the ordination of sites (i.e., where sites predicted by the metrics to have long hydroperiod under free flowing conditions represent locations where anthropogenic activities have in fact shortened hydroperiod) highlights an important consideration when applying these metrics for pattern assessment, and is evident in the location of specific sites along the gradient of predicted hydroperiod (Fig. 7). For example, blocks P20, P28 and P108 are located in WCA3B where actual hydroperiods have been dramatically shortened by the network of canals and levees; all three metrics predict long hydroperiod. We interpret this to mean that the pattern that has emerged in these blocks would, under free-flowing conditions, lead to long hydroperiods, which, in turn, would lead to reductions in ridge density. Similarly, P2 is located in an area north of Tamiami Trail in WCA3A where hydroperiod is artificially prolonged. Vegetation adjustments in response to those existing hydrologic conditions have created a pattern that would, under free-flowing conditions, have a very short hydroperiod (i.e., higher discharge competence and connectivity), leading eventually to ridge expansion. Notably, sites with intermediate predicted hydroperiod (P0, P4, P7) correspond to those areas where pattern is best conserved, further reinforcing the conclusion that metrics capture how vegetation pattern adjusts to imposed hydrological changes where they have occurred.

Limitations and utility for Everglades monitoring

The application of a single discharge time series to each model domain boundary is an important limitation of our work. The remnant Everglades are characterized by significant spatial variation in flow regimes, and patterning changes can largely be linked to these hydrologic modifications. However, while the Everglades is replete with stage information (e.g., the Everglades Depth Estimation Network, EDEN; http://sofia.usgs.gov/eden/), translating these stage time-series to associated time-series of discharge requires significant effort, and the development of these rating curves is confounded by the presence of flow control structures and levees that create significant back-water effects (i.e., where stage and flow are uncorrelated). As such, we considered only the single 20-year time series of flow obtained from an analysis of existing stage data in the best conserved regions of the ridge-slough landscape. We note, however, that this 20-year record has considerable within- and across-year variation in discharge, which highlights some of the key drivers of landscape conditions (specifically, the critical role of variation in low flow periods across years, which controls variation in ridge hydroperiod; Kaplan et al. 2012).

While the metrics proposed are apparently effective at capturing variation in extant pattern, both in time and space, they are based on 2-dimensional patterns, and thus may fail to capture degradation in the vertical dimension as divergence in soil elevation between ridges and sloughs degrades (Watts et al. 2010). Vertical differentiation between patch types occurs in response to vegetation inputs of litter (production) and organic matter mineralization (respiration), both of which vary with mean water depth (Larsen et al. 2007; Watts et al. 2010; Heffernan et al. 2013), creating two patch types (ridges and sloughs) that achieve the same long-term peat accretion. Crucially, spatial surveys of soil elevation (Watts et al. 2010) suggest that loss of divergence (i.e., transition from bimodal to unimodal soil elevation distributions) may occur faster than changes in vegetation pattern. This could create situations where all pattern metrics used to diagnose the health of ecosystem fail to detect early onset of important ecological changes. Future work on pattern metrics is needed to link two-dimensional metrics to soil elevation indices, and to determine where in the trajectory of ecological change each indicator becomes sensitive.

We also note that the onset of hydrologic modification occured long before the first availability of aerial surveys from which pattern can be obtained.

Hydrologic alteration in the Everglades started in the 19th century (Light and Dineen 1994), rendering hindcast conditions far from pristine. As such, we cannot interpret the estimated historical hydroperiod as representative of free-flowing conditions when structures are absent. For example, all of the sites in WCA3B (the triangular area to the southeast of WCA3, including plots I4, I5 and NG; Fig. 2) have landscape patterns over the entire period of record that would, under free flowing conditions result in very long hydroperiod (Fig. 7b). We interpret this to mean that vegetation has reorganized in response to prolonged drydown, the onset of which predated our 1941 maps. In contrast, sites G3 and N5 are at the southern end of WCA3, and have been impacted by Tamiami Trail since it was constructed in 1928. The significant downward trajectory of the free-flowing hydroperiod response suggests that this area has been reorganizing in response to prolonged inundation for the entire period of record, which may reflect ongoing and slow transition to a new landscape equilibrium. There are also patterns that run counter to expectations. For example, there is no detectable trend in hydroperiod in the northern part of WCA3 with the exception of the I1 block despite significantly reduced hydroperiod in that block over the period of record. This finding comports with the complex and highly variable pattern changes observed by (Nungesser 2011). Limited temporal resolution of vegetation maps may confound generalizations of landscape change, and call for finer temporal resolution information, perhaps via regular satellite images analysis.

One intriguing question that arises is how much the predicted hydroperiod changes in response to landscape scale vegetation changes. In other words, how does the effect of ridge density on hydroperiod change across metrics, and across landscape condition (i.e., initial ridge density)? The sensitivity of hydrology to landscape condition, a property we refer to as the landscape adaptive capacity, is critical for assessing the trajectory of landscape responses to hydrologic modification and restoration. To explore this property, we plotted observed changes in ridge density (Δ%R) in each landscape block from one date to the next against the associated change in predicted hydroperiod (ΔHP). We then classified each point based on the initial ridge density (<60, <70, <80 and >80 %), and evaluated the slope and fit of the Δ%R versus ΔHP line (Fig. 9). The results suggest that landscapes adaptive capacity declines strongly with increasing initial ridge density. For all metrics, the fitted slopes, which quantify the landscape adaptive capacity, are lower at higher initial density. For LFC, this change is relatively modest, with slopes declining by 50 % over the 4 density categories; model fit was good across categories. In contrast, LDC and DCI exhibit far more dramatic declines in slope, and marked reductions in model fit, with higher initial ridge density. While there is strong agreement across metrics that the same extent of vegetation change (e.g., a 5 % change in ridge density) has different impacts on hydrology depending on initial conditions, the metrics disagree regarding the magnitude of this effect. We note than above LFC values of 1.1, predicted changes in HP are small (Fig. 7a), explaining the diminishing effect of additional ridge pixels as the total proportion of ridges increases. The relationship between DCI and HP is more complex (Fig. 7b), which may explain the steepest slopes in Fig. 9 at intermediate density. Finally, the relationship for LDC, which weakens dramatically with increased density, likely arises because of the particular formulation (e:%R) which creates the largest effects of e at low ridge densities. Together, these behaviors suggest that the reciprocal feedback expected between pattern and hydroperiod under free-flowing conditions (Kaplan et al. 2012) will be strongest at low ridge density, and weaken dramatically with increased density. This may mean that landscapes where ridge density has increased dramatically are resistant to restoration arising from self-organized hydroperiod effects alone.

Designing and using metrics that explicitly link pattern to hydrology are of particular relevance as performance measures for assessing restoration and degradation trajectories (Restoration Coordination and Verification (RECOVER) 2006b; NRC 2006). The need for performance measures that enumerate the health of the ridge-slough landscape has been clearly identified in the comprehensive Everglades restoration plan (CERP) because this patterned landscape is the largest component of the historical system and is integral as habitat and flow conveyance. While a suite of performance measures has been developed including hydrological, biological/ecological metrics (Doren et al. 2009), pattern metrics developed from remote sensing images have several important advantages compared to biological indices, principally related to the scale and repeatability of measurements.

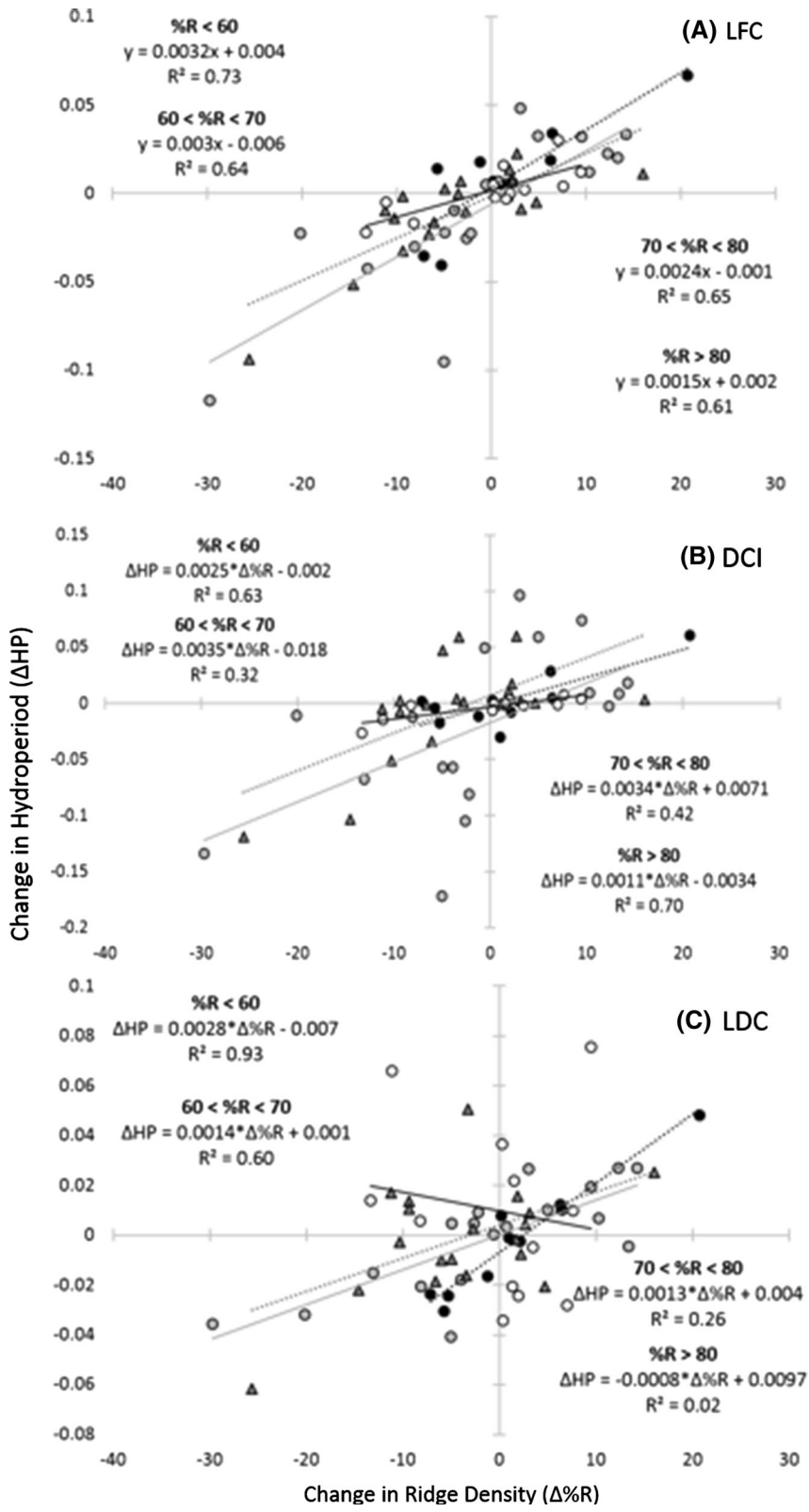

Fig. 9 Across all three metrics, there are differential effects of changes in ridge density (Δ%R) on changes in predicted hydroperiod (ΔHP) depending on initial ridge density. However, the effects of ridge density changes are most consistent across initial ridge density for LFC and least consistent for LDC

Our principal conclusion in this work is that metrics like DCI and LFC, which are both easy to obtain and explicitly consider hydrological processes and their links to pattern, have considerable utility as restoration performance measures.

Acknowledgments We would like to thank Likai Zhu for his assistance in Python programming and R scripting. Danielle Watts, Jim Heffernan, Joseph Delesantro, Stephen Casey and Jim Jawitz have all been invaluable resources for discussing the ideas presented in this work. We also acknowledge the constructive inputs from two anonymous reviewers whose suggestions greatly improved the paper.

References

Aich S, McVoy CW, Dreschel TW, Santamaria F (2013) Estimating soil subsidence and carbon loss in the Everglades Agricultural Area, Florida using geospatial techniques. Agric Ecosyst Environ 171:124–133

Bullock A, Acreman M (1999) The role of wetlands in the hydrological cycle. Hydrol Earth Syst Sci 7(3):358–389

Burnham KP, Anderson DR (2002) Model selection and multimodel inference: a practical information-theoretic approach. Springer, New York

Cheng Y, Stieglitz M, Turk G, Engel V (2011) Effects of anisotropy on pattern formation in wetland ecosystems. Geophys Res Lett 38(4):L04402

Cohen M, Watts D, Heffernan J, Osborne T (2011) Reciprocal biotic control on hydrology, nutrient gradients, and landform in the greater Everglades. Crit Rev Environ Sci Technol 41:395–429

Corry RC, Nassauer JI (2005) Limitations of using landscape pattern indices to evaluate the ecological consequences of alternative plans and designs. Landsc Urban Plan 72(4):265–280

D'Odorico P, Engel V, Carr JA, Oberbauer SF, Ross MS, Sah JP (2011) Tree-grass coexistence in the everglades freshwater system. Ecosystems 14(2):298–310

Deutsch CV, Journel AG (1998) GSLib. Geostatistical software library and user's guide

D'Odorico P, Laio F, Porporato A, Ridolfi L, Rinaldo A, Rodriguez-Iturbe I (2010) Ecohydrology of terrestrial ecosystems. Bioscience 60(11):898–907

Doren RF, Trexler JC, Gottlieb AD, Harwell MC (2009) Ecological indicators for system-wide assessment of the greater everglades ecosystem restoration program. Ecol Ind 9(6):S2–S16

Eastman JR (1989) Pushbroom algorithms for calculating distances in raster grids. In: Proceedinds of Autocarto, vol. 9, pp 288–297

Eastman JR (1990) IDRISI: a grid-based geographic analysis system. Clark University, Graduate School of Geography

Egler FE (1952) Southeast saline Everglades vegetation, Florida and its management. Vegetatio 3(4–5):213–265

Eppinga MB, Rietkerk M, Borren W, Lapshina ED, Bleuten W, Wassen MJ (2008) Regular surface patterning of peatlands: confronting theory with field data. Ecosystems 11(4): 520–536

Eppinga MB, de Ruiter PC, Wassen MJ, Rietkerk M (2009) Nutrients and hydrology indicate the driving mechanisms of peatland surface patterning. Am Nat 173(6):803–818

Givnish TJ, Volin JC, Owen VD, Volin VC, Muss JD, Glaser PH (2008) Vegetation differentiation in the patterned landscape of the central Everglades: importance of local and landscape drivers. Glob Ecol Biogeogr 17(3):384–402

Gustafson EJ (1998) Quantifying landscape spatial pattern: what is the state of the art? Ecosystems 1(2):143–156

Hagerthey SE, Newman S, Rutchey K, Smith EP, Godin J (2008) Multiple regime shifts in a subtropical peatland: community-specific thresholds to eutrophication. Ecol Monogr 78(4):547–565

Harvey J, Schaffranek R, Noe G, Larsen L, Nowacki D, O'Connor B (2009) Hydroecological factors governing surface water flow on a low-gradient floodplain. Water Resour Res 45(3)

Heffernan JB, Watts DL, Cohen MJ (2013) Discharge competence and pattern formation in peatlands: a meta-ecosystem model of the Everglades ridge-slough landscape. Plos One 8(5):e64174

Kaplan DA, Paudel R, Cohen MJ, Jawitz JW (2012) Orientation matters: patch anisotropy controls discharge competence and hydroperiod in a patterned peatland. Geophys Res Lett 39(17)

Kupfer JA (2012) Landscape ecology and biogeography: rethinking landscape metrics in a post-FRAGSTATS landscape. Progr Phys Geogr. ISSN 0309133312439594

Lago ME, Miralles-Wilhelm F, Mahmoudi M, Engel V (2010) Numerical modeling of the effects of water flow, sediment transport and vegetation growth on the spatiotemporal patterning of the ridge and slough landscape of the Everglades wetland. Adv Water Resour 33(10):1268–1278

Larsen L, Harvey J, Crimaldi J (2007) A delicate balance: ecohydrological feedbacks governing landscape morphology in a lotic peatland. Ecol Monogr 77(4):591–614

Larsen LG, Harvey JW (2010) How vegetation and sediment transport feedbacks drive landscape change in the Everglades and wetlands worldwide. Am Nat 176(3):E66–E79

Larsen LG, Choi J, Nungesser MK, Harvey JW (2012) Directional connectivity in hydrology and ecology. Ecol Appl 22(8):2204–2220

Light SS, Dineen JW (1994) Water control in the Everglades: a historical perspective. In: Davis SM, Ogden JC (eds) Everglades: the ecosystem and its restoration. St. Lucie Press, Delray Beach, pp 47–84

Ludwig JA, Eager RW, Bastin GN, Chewings VH, Liedloff AC (2002) A leakiness index for assessing landscape function using remote sensing. Landscape Ecol 17(2):157–171

Ludwig JA, Eager RW, Liedloff AC, Bastin GN, Chewings VH (2006) A new landscape leakiness index based on remotely sensed ground-cover data. Ecol Ind 6(2):327–336

McGarigal K, Cushman SA, Neel MC, Ene E (2002) FRAGSTATS: spatial pattern analysis program for categorical maps

McVoy CW, Park WA, Obeysekera J, VanArman J, Dreschel TW (2011) Landscapes and hydrology of the pre-drainage Everglades. University Press of Florida, Gainesville

National Research Council (NRC), Progress toward restoring the everglades: the first biennial review (2006) Committee on independent scientific review of everglades restoration progress (CISRERP). National Academies Press, Washington, DC

Nungesser M (2011) Reading the landscape: temporal and spatial changes in a patterned peatland. Wetlands Ecol Manage 19(6):475–493

O'Neill RV, Riitters KH, Wickham JD, Jones KB (1999) Landscape pattern metrics and regional assessment. Ecosyst Health 5(4):225–233

Opdam P, Foppen R, Vos C (2001) Bridging the gap between ecology and spatial planning in landscape ecology. Landscape Ecol 16(8):767–779

Reddy KR, Diaz OA, Scinto LJ, Agami M (1995) Phosphorus dynamics in selected wetlands and streams of the Lake Okeechobee Basin. Ecol Eng 5(2):183–207

Restoration Coordination and Verification (RECOVER) (2006b) Report on Evaluation Tools, Models, Work Plans, and Budgets. c/o U.S. Army Corps of Engineers Jacksonville District, Jacksonville, FL, and South Florida Water Management District, West Palm Beach

Rietkerk M, Van de Koppel J (2008) Regular pattern formation in real ecosystems. Trends Ecol Evol 23(3):169–175

Ross MS, Mitchell-Bruker S, Sah JP, Stothoff S, Ruiz PL, Reed DL, Jayachandran K, Coultas CL (2006) Interaction of hydrology and nutrient limitation in the Ridge and Slough landscape of the southern Everglades. Hydrobiologia 569:37–59

Rutchey K, Vilchek L (1999) Air photointerpretation and satellite imagery analysis techniques for mapping cattail coverage in a northern Everglades impoundment. Photogramm Eng Remote Sens 65(2):185–191

Rutchey K, Schall TN, Doren RF, Atkinson A, Ross MS, Jones DT, Madden M, Vilcheck L, Bradley KA, Snyder JR, Burch JN, Pernas T, Witsher B, Pyne M, White R, Smith III TJ, Sadle J, Smith CS, Patterson ME, Gann GD (2006) Vegetation classification for South Florida Natural Areas. US Geological Survey, Open-File Report 2006–1240, St. Petersburg, Florida, p 142

Rutchey K, Schall T, Sklar F (2008) Development of vegetation maps for assessing Everglades restoration progress. Wetlands 28(3):806–816

Schaffranek RW (2004) Simulation of surface-water integrated flow and transport in two-dimensions: SWIFT2D User's Manual. US Department of the Interior, US Geological Survey

SCT (2003) The role of flow in the Everglades ridge and slough landscape. Science Coordinating Team, South Florida Ecosystem Restoration Working Group, Miami, FL, USA. https://sofia.usgs.gov/publications/papers/sct_flows/

Sklar FH, van der Valk A (2002) Tree islands of the Everglades. Springer, New York

Suding K, Gross K, Houseman G (2004) Alternative states and positive feedbacks in restoration ecology. Trends Ecol Evol 19(1):46–53

Tongway DJ, Ludwig JA (1997) The conservation of water and nutrients within landscapes. In: Ludwig J, Tongway D, Freudenberger D, Noble J, Hodgkinson K (eds) Landscape ecology, function and management: principles from Australia's rangelands. CSIRO publishing, Melbourne, pp 13–22

Turner MG (1989) Landscape ecology: the effect of pattern on process. Ann Rev Ecol Syst 29:171–197

Turner MG, Gardner RH, O'Neill RV (2001) Landscape ecology in theory and practice: pattern and process. Springer, New York

Watts D, Cohen M, Heffernan J, Osborne T (2010) Hydrologic modification and the loss of self-organized patterning in the ridge-slough mosaic of the Everglades. Ecosystems 13(6):813–827

Willard DA, Bernhardt CE, Holmes CW, Landacre B, Marot M (2006) Response of Everglades tree islands to environmental change. Ecol Monogr 76(4):565–583

Wu J, Hobbs R (2002) Key issues and research priorities in landscape ecology: an idiosyncratic synthesis. Landscape Ecol 17(4):355–365

Wu Y, Wang N, Rutchey K (2006) An analysis of spatial complexity of ridge and slough patterns in the Everglades ecosystem. Ecol Complex 3(3):183–192

Yuan J (2015). Metrics of pattern loss and ecosystem change in the ridge and slough mosaic of the Everglades. Retrieved from ProQuest Dissertations and Theses (Accession Order No. AAT)